World Journal of Microbiology and Biotechnology (2020) 36:141
https://doi.org/10.1007/s11274-020-02915-1

ORIGINAL PAPER

Integration between bacterial consortium and magnetite (Fe_3O_4) nanoparticles for the treatment of oily industrial wastewater

Ebtesam El Bestawy[1] · Basma Farg El-Shatby[1] · Abdelazeem Saad Eltaweil[2]

Received: 21 March 2020 / Accepted: 11 August 2020 / Published online: 19 August 2020

Abstract

The study aimed to investigate the efficiency of exogenous bacterial consortium (*Enterobacter cloacae* and *Pseudomonas otitidis*) decorated (immobilized) with Fe_3O_4 Nanoparticles for the treatment of petroleum hydrocarbon-contaminated wastewater. Glycine coated magnetite Nanoparticles (Fe_3O_4 NPs) were prepared using reverse co-precipitation method and were characterized using X-ray diffraction, transmission and scanning electron microscopy and vibrating sample magnetometer. They were used to decorate exogenous bacterial consortium (*Enterobacter cloacae* and *Pseudomonas otitidis*) at 3 different Fe_3O_4/bacteria ratios (1:1, 1:3 and 3:1 w/w). Bioremediation of oil contaminated wastewater collected from one of the petroleum distribution companies, Alexandria was conducted for 168 h using Fe_3O_4/bacterial association at the best ratio (3:1) and compared with non-decorated consortium and the indigenous bacteria in the control. Analysis indicated crystalline structure of Fe_3O_4 NPs with spherical particles (size: 15–20 nm) and superparamagnetic properties. Glycine modified-Fe_3O_4 exhibited high ability to immobilize bacteria which acquired its magnetic properties. The highest coating efficiency (92%) was achieved at 3:1 Fe_3O_4/bacteria ratio after 1 h. This ratio positively affected bacterial growth reaching the highest growth rate (5.07 fold higher than the control) after 4 h. The highest removal efficiencies of the total suspended solids (TSS), chemical oxygen demands (COD), oil and grease (O&G) and total petroleum hydrocarbons (TPH) recording 96, 65.4, 83.9 and 85% reaching residual concentrations of 9.5, 598, 99 and 60 mg/l respectively were achieved after 4 h by the Fe_3O_4-bacteria assembly. Compared with the maximum permissible limits of the tested parameters, TSS residue was highly compiled with its limit (50 mg/l), while COD, O&G and TPH were 7.5, 9.9, and 120-folds higher than their limits (100, 15 and 0.5 mg/l respectively). To the best of our knowledge it is first time to use integrated *Enterobacter cloacae* and *Pseudomonas otitidis* consortium decorated with Fe_3O_4 NPs for the treatment of petroleum hydrocarbon-contaminated wastewater. The proposed system proved to be a very efficient, economical and applicable for the removal of the included contaminants in very short running time which increases its biotechnological added value.

Keywords Bacteria · *Enterobacter cloacae* · Immobilization · Magnetite Nanoparticles · Petroleum Hydrocarbons · *Pseudomonas otitidis* · Wastewater Treatment

Introduction

Petroleum oil industrial processes (manufacturing, cleaning activities or leakages) generate a variety of pollutants which have negative environmental impacts due to their toxicity, carcinogenic and mutagenic properties

Electronic supplementary material The online version of this article (doi:https://doi.org/10.1007/s11274-020-02915-1) contains supplementary material, which is available to authorized users.

✉ Ebtesam El Bestawy
ebtesamelbestawy@yahoo.com

✉ Abdelazeem Saad Eltaweil
abdelazeemeltaweil@alexu.edu.eg

Basma Farg El-Shatby
basma.elshatby@gmail.com

[1] Department of Environmental Studies, Institute of Graduate Studies and Research, Alexandria University, 163 Horria Ave. El-Shatby, P.O. Box 832, Alexandria, Egypt

[2] Department of Chemistry, Faculty of Science, Alexandria University, Alexandria, Egypt

(Changmai et al. 2019; Qiao et al. 2019). Oil-contaminated ecosystems might take years or even decades to be recovered, therefore, treatment and safe discharge has always been a significant and critical environmental issue (Chen et al. 2020). Oily wastewater releases unwanted toxins into the air, soil and receiving aquatic resources (drinking water, groundwater and open oceans or rivers) worldwide, and threatening human health since it contains a mixture of complex aliphatic, aromatic, asphaltene and resin hydrocarbons, all of which are well reported as toxic, mutagenic and carcinogenic in nature (Soares-Castro et al. 2019; Tanudjaja et al. 2019). They are also affecting crop production, destructing natural landscape and causing safety problems as oil burning (Poulopoulos et al. 2005; Yu et al. 2017) as well as exerting great risk to all biotic and abiotic components of the environment. Phenolic compounds (Pardeshi and Patil 2008; Abdelwahab et al. 2009; Diya'uddeen et al. 2011) and many polycyclic aromatic hydrocarbons (PAHs) (Al Zarooni and Elshorbagy 2006) that may exist in refinery wastewater with naphthalene are highly carcinogenic, toxic, stable, more persistent in the environment and bioaccumulated in the food chain while many sulfur compounds (hydrogen sulfide, mercaptans and disulfides) present in the crude oil must be adjusted in the final products to percentage in the limits permitted by standards and environmental regulations (Yu et al. 2018). Sulfide contributes to oxygen depletion since it has a high oxygen demand (Rathnayake et al. 2019), thus, results in mass fish mortality when the threshold limit exceeds 0.5 mg/l for freshwater or saltwater fish (Henshaw and Zhu 2001; Altaş and Büyükgüngör 2008). Refinery wastewater characterized by lower BOD due to the nature of the partially biodegradable organic materials while has high COD since it measures the total required amount of oxygen to chemically oxidize all organic matter (Chen et al. 2018). In discharge distribution system sticky oil and grease (O&G) tend to aggregate, clogging drain pipes and sewer lines and causing unpleasant odours and corroding sewer lines under anaerobic conditions (Stoll and Gupta 1997). While inside the treatment plants, they float on the top of the water, block strainers and filters and reduce biological activity (microbial oxidation) of organic molecules (Xu and Zhu 2004). O&G have mutagenic and carcinogenic effects on human and aquatic organisms (plant and animal). In the open environment, O&G layer on the water surface decreases atmospheric dissolved oxygen interchange which damages the ecology of the receiving water bodies. TPHs represent both soluble and insoluble parts with variable solubility in water where paraffinic hydrocarbons have a very low solubility in water, while aromatic hydrocarbons are more soluble (Polak and Lu 1973).

Biological treatment of wastewater is advantageous over physical–chemical treatment because of its low cost, environmentally friendly approach and the ability of using microbial enzymes and biosurfactants in degrading (converting) organic pollutants into harmless substances (Wang and Fingas 1995; El-Bestawy et al. 1998; El Bestawy et al. 2014; Crini and Lichtfouse 2019; Liu et al. 2019b). Immobilized (fixed) microbial cells are preferred than suspended cells due to their operational stability against adverse environmental conditions (temperature and pH), high mechanical strength, high metabolic activity, easier separation and the ability to be reused (Hou et al. 2016; Katam and Bhattacharyya 2019).

Oily wastewater is complex and using a single-treatment method is difficult to achieve national emission standards for industrial wastewater, therefore, integrated technologies are preferred (Yu et al. 2017). A new technique was developed where microbial cell surfaces are coated with magnetic Nanoparticles (NPs) through strong physical adsorption due to the high specific surface area and high surface energy of NPs (Darabdhara et al. 2017). The smaller size of the NPs increases the surface area which enhances chemical activity and capacity of NPs for adsorbing many types of pollutants on their surface (Gubin et al. 2005; Kalfa et al. 2009). NPs and bacterial cells integration assisting microbial activities and increase their reaction rates whereas magnetic NPs attached onto microbial cells, can easily be detached from the medium after complete treatment using external magnetic field for reuse (Shan et al. 2005; Ranmadugala et al. 2018). NPs and bacterial cells integration can overcome technological limitations such as reduced solubility of hydrophobic substrate, reduced bioavailability to the microorganisms, kinetic limitations on crude oil degrading enzymes, un-healthy microorganisms (Kumari and Singh 2016; Baghaie and Jabari 2019), drawbacks of biomass loading limitation, loss of cells from the carrier in case of conventional immobilization by adsorption and eliminating mass transfer problems associated with the common entrapment methods and reusing the cells (Escobar et al. 2019).

NPs coated bacterial cells assemblages have been extensively investigated for the removal of different pollutants during wastewater treatment where they may show higher or similar activity as their non-coated bacteria. For example, *Rhodococcus erythropolis* IGST8- Fe_3O_4 nanoparticles assemblage (modified with glycine) could achieve 56% higher biodesulfurization (BDS) of dibenzothiophene (DBT) in basic salt medium (BSM) compared to the non-decorated cells. Nanoparticles indeed enhance bacterial membrane permeability which facilitated the entry and exit of reactants and products, respectively (Ansari et al. 2009). Similarly, Glycine-Al_2O_3 Nano sorbents assembled on the surfaces of *Pseudomonas delafieldii* R-8 cells, a desulfurization strain have selective ability to adsorb dibenzothiophene (DBT) from oil phase. Thus, DBT can be quickly transferred to the biocatalyst surface where Nano sorbents were located which increases biodesulfurization rate. The desulfurization rate of the cells

assembled with Nano sorbents was approximately two fold higher than that of original cells (Guobin et al. 2005). Bacterial species considered a critical factor determining the efficiency of the microbial/NPs assemblage. In that regard, strains such as *Pseudomonas delafieldii* (Shan et al. 2005), *Rhodococcus erythropolis* FMF and *R. erythropolis* IGTS8 (Bardania et al. 2013), *Rhodococcus erythropolis* LSSE8-1 (Li et al. 2009) coated with magnetic Fe_3O_4 nanoparticles showed similar desulfurization activity with their non-coated cells. However, they exhibited high operational stability, easy separation from fermentation broth by magnetic force and high reusability (more than five cycles) with the same bacteria.

Magnetic cells also used in the removal of heavy metals from wastewater. The huge amount of copper-laden waste production which is the highest among all heavy metals in Hong Kong was studied by a copper-resistant bacterial strain, *P. putida* 5X which was immobilized using magnetite Fe_3O_4 to remove large amount of Cu^{+2} from electroplating effluent. The removal capacity of the immobilized cells could reach 14 mg Cu^{+2}/g immobilized dry cells under optimal conditions (Sze et al. 1997). Also, usage of nanoparticles was shown effective and a unique tool for rapid pathogen detection, decontamination, and strain differentiation without time-consuming cell culturing. Magnetic glyconanoparticles (MGNPs)-based system detects *E. coli* within 5 min and removes up to 88% of the target bacteria from the medium. Furthermore, the identities of three different *E. coli* strains were easily determined on the basis of their response patterns to two MGNPs highlighting their potential in biosensing (El-Boubbou et al. 2007). Herein, the present study aimed to develop a new magnetite-coated bacterial assemblage as an efficient and magnetically separable system for the treatment of oily industrial wastewater.

Materials and methods

Sampling

Samples were collected from the final drainage effluent of one of the petroleum distribution companies, Alexandria, Egypt during the course of the present study. Oily wastewater samples were subjected to physicochemical as well as microbiological characterization to define their pollution strength and selecting the best treatment technology. In addition, post-treatment characterization took place in order to calculate the treatment efficiency.

Microorganisms

Two bacterial strains namely *Enterobacter cloacae* NCDC279-56 (ATCC 13047) and *Pseudomonas otitidis* MCC10330 (ATCC BAA-1130) were selected out of six pure exogenous cultures which exhibited superior ability for degradation of not only oil hydrocarbons but other contaminants included in petroleum-contaminated wastewater as shown in Supplementary data (S1). They were kindly provided from IGSR (Institute of Graduate Studies & Research, Alexandria University) collection and originally isolated from heavily polluted soil and also exhibited superior ability for organic matter, pesticides and heavy metals removal. In the present study, they were investigated as consortium, either as free living culture or as Fe_3O_4 NP-bacterial consortium assembly, for their ability to bioremediate contaminated wastewater from petroleum industry.

Synthesis of magnetite NPs

Magnetite NPs were synthesized using reverse co-precipitation method under N_2 stream during the whole preparation steps (Sulistyaningsih et al. 2017). In details, 5.2 g of $FeCl_3{\cdot}6H_2O$ and 2.674 g of $FeSO_4{\cdot}7H_2O$ were dissolved in 50 ml deionized water and stirred for 15 min under inert atmosphere at room temperature. Ammonia solution (25%) was added to the mixture till pH ~ 10 under continuous stirring for another 30 min to achieve nucleation and formation of magnetite nanoparticles. Glycine (1.2 g) was added to the magnetite NPs (Fe_3O_4) as a surfactant to stabilize their dispersion. The black solid product was sonicated using ultrasonic bath for 20 min. Magnetite NPs were isolated from the solution using an external magnet, washed three times with deoxygenated water and ethanol then dispersed and stored in ethanol. Formation of Fe_3O_4 NPs followed the equation:

$$2FeCl_3 + FeSO_4 + 4H_2O + 8NH_3 \rightarrow Fe_3O_4 + (NH_4)2SO_4 + 6NH_4Cl \quad (1)$$

Characterization of magnetite NPs

The prepared magnetic NPs were characterized by different tools to explore their chemical, morphological and magnetic properties. Transmission electron microscope (JEOL, JEM 100 CX, Japan) and scanning electron microscope (SEM-JEOL JSM-IT 200, Japan) were used to determine particles size and morphology of the prepared NPs as well as magnetic-coated bacteria. Crystal phase was examined using X-ray diffractometer (XRD BRUKER D8 Advance Cu target, Germany), operating with CuKα radiation (λ = 1.54 A°) generated at 40 kV and 40 mA. Room temperature magnetic characteristics of the nanoparticles were determined by using a vibrating sample magnetometer (VSM) in an external magnetic field of 20 KG (20 KOe). The functional groups of the magnetic NPs as well as the NPs-Coated bacteria were examined using Fourier Transform Infrared Spectroscopy (FT-IR, Model 8400 S, Shimadzu, Japan). It

was performed in order to identify organic functional groups present on the NPs as well as the molecular interactions between the adsorbed molecules and the NPs.

Development of the NPs-coated bacterial assemblage system (immobilization of magnetite onto bacterial cells)

The selected mixed culture {*Enterobacter cloacae* NCDC279-56 (ATCC 13047) and *Pseudomonas otitidis* MCC10330 (ATCC BAA-1130)} was grown on nutrient broth (NB) medium for 24 h at 37 °C till cell density of ~ 1.7 g/l (dry weight). Then, fixed volumes of the mixed cultures (5 ml each = 0.0085 g) were mixed with various amounts of magnetite (0.0028, 0.0085 and 0.0255 g; i.e. 145, 436 and 1308 µl from the stock magnetite solution 19.5 g/l) equivalent to magnetite-bacterial consortium assembly (g/g) ratios of 1:1, 1:3 and 3:1 (A, B and C, respectively) using shaking incubator at 180 rpm (New Brunswick Scientific, NJ, USA) at 37 °C.

Evaluation of NPs Immobilization onto Bacterial Cells and Effect on their Growth

After 1 h, magnetite NPs coated bacterial cells were separated by an external magnetic field and the resulting supernatant was then harvested which represents free uncoated cells. Cell density of the free uncoated bacteria (supernatant) and total cells (before the separation of the magnetic bacterial cells with an external magnet) were determined using UV/Vis spectrophotometer (Lambda Bio40, Perkin–Elmer Instruments, USA) at OD_{600}. The above mentioned procedure was repeated after 15 h to check the stability of the immobilization (NPs-Bacteria Assemblage) (Li et al. 2009; Reddy et al. 2012; Raee et al. 2019). The efficiency of coating/immobilization (%E) was evaluated according to the following equation:

$$\%E = \frac{OD_{600(\text{total cells})} - OD_{600(\text{uncoatedcells})}}{OD_{600(\text{total cells})}} \quad (2)$$

where OD = Optical density at λ = 600 nm.

Moreover, effects of Fe_3O_4 NPs on the growth of bacteria: Fe_3O_4 cultures (at the 3 tested ratios) as well as control culture (magnetite-free) were investigated using cell densities determined in the previous step at different retention time (0, 2, 4, 15 and 19 h). Two blanks were used for measurement of the absorbance, one for the total dosed cells (composed of bacteria free-NB medium with magnetite only at the same concentrations used) and the second blank for control culture (composed of bacteria free-NB medium). At each exposure time, drawn samples were diluted to 10^{-1} before measurement. Growth rate of the Fe_3O_4 amended cultures were also compared with the control culture (Kafayati et al. 2013).

Treatment Using Fe_3O_4-Bacteria Assembly

The selected bacterial consortium was inoculated in NB medium and incubated for 24 h at 37 °C till heavy growth was obtained (~1.4 g DW/L). Magnetite NPs-bacteria assembly was prepared at the perfect ratio (3:1 w/w) that exhibited the highest coating efficiency (immobilization) and the highest bacterial growth rate. This was performed by mixing 105 ml of magnetite (2.025 g) and 500 ml bacterial culture (0.675 g) using rotary shaker at 180 rpm and 37 °C for 1 h to confirm the coating process before augmentation into hydrocarbon contaminated effluent (2.5 L). In addition, magnetite-free mixed culture (500 ml of 24 h NB consortium culture) and 2.5 L unseeded wastewater were run as controls in a batch mode parallel and under the same conditions with magnetite–bacteria assembly culture. Magnetite amended culture, magnetite-free culture and the unseeded wastewater (control) were incubated under shaking (180 rpm) at 37 °C for 168 h. During the first 4 h, samples were aseptically drawn at 1 h interval after which samples were taken after 24, 120 and 168 h to examine their ability and behaviour after longer exposures. Bacterial growth rate was measured as optical density (OD) along the experiment duration starting from the initial inoculation (starting point). Raw and treated effluents were characterized for dissolved oxygen (DO), COD, BOD, TSS, total dissolved solids (TDS), total viable count of bacteria (TVC), O&G and TPH to determine their residual levels, removal efficiency and compare among them.

Treatment using magnetite NPs

To determine whether the obtained results is caused by the presence of magnetite NPs or the magnetite-bacteria assembly during the treatment process, the same treatment of oily wastewater was repeated under exactly the same conditions using bacteria free-magnetite NPs and magnetite-microbial cells assembly separately and a comparison was made.

Characteristics of the raw and treated industrial effluent

Petroleum contaminated wastewater was characterized before and after the proposed treatment. Quality parameters of the wastewater included its pH, temperature, DO, TDS,

TSS, COD, O&G, TPH and TVC, all of which were determined using the standard techniques described in the Standard Methods for the Examination of Water and Wastewater (Clesceri et al. 1999). After treatment, removal efficiency (RE) of the selected parameters at each exposure time was calculated from their residual levels to determine the effectiveness of the remediation process.

Statistical analysis

Mean (3 replicates) and standard error values were determined for all the parameters and the results were expressed as mean ± standard error. Data were analyzed using one-way analysis of variance (ANOVA) followed by Duncan multiple comparison {Statistical Package for the Social Sciences program (SPSS) for windows (Version 20)} in order to compare treated groups with control and also to compare treatment using Fe_3O_4-immobilized bacteria at different exposure times (S2A and B). The differences were considered significant at $P < 0.05$ (95% of the confidence level). In addition, Pearson Correlations were calculated among the different contaminants present in the petroleum hydrocarbon contaminated effluents during Fe_3O_4-immobilized bacteria bioassay (S2C).

Results

Enterobacter cloacae NCDC279-56 and *Pseudomonas otitidis* MCC10330 were investigated for the treatment of hydrocarbon contaminated effluent as Fe_3O_4-immobilized and Fe_3O_4-free consortium cultures.

Characterization of magnetic NPs

X-ray diffraction

Crystalline structure of magnetite was investigated by XRD technique (Fig. 1a). Magnetite standard characteristic peaks at $2\theta = 35.5°$, 29.8°, 62.7°, 43°, 57.2°, 53.7° and 73.8° are observed. Diffraction peaks are attributed to cubic phase structure of magnetite according to JCPDS card, No. 01-089-0691. The diffractogram showed that there was no formation of other types of iron oxides. The XRD patterns of magnetite NPs also indicated that the NPs are well crystallized.

Vibrating sample magnetometer (VSM)

Magnetic property of the pure magnetite NPs was examined using VSM and the typical room temperature magnetization curve of magnetite is shown in Fig. 1b. Saturation magnetization (Ms) recorded 39.96 emu/g with remnant

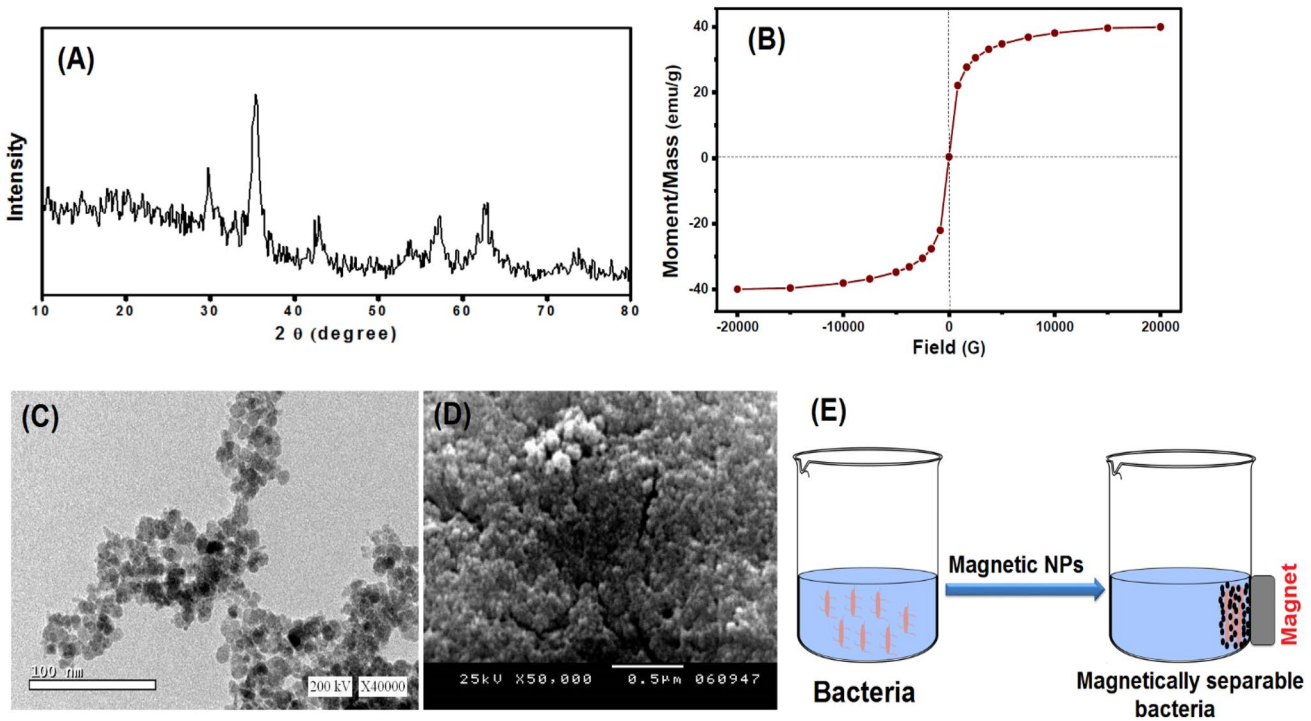

Fig. 1 Characterization of magnetite NPs: X-ray diffraction pattern (**a**), Vibrating sample magnetometer (**b**), TEM image (**c**), SEM image (**d**) of Fe_3O_4 nanoparticles and schematic representation for the formation of magnetically separable magnetic NPs-coated bacteria (E)

magnetization (Mr) of 7.34 emu/g and the coercivity (Hc) approaches zero (0.30 emu/g) which reflects that the prepared magnetite NPs have superparamagnetic behaviour.

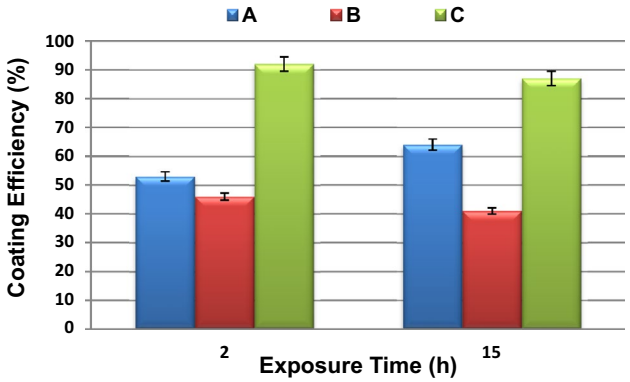

Fig. 2 Coating efficiency (%) of different magnetite doses on bacteria at different exposure times where A, B and C represent magnetite-bacterial consortium ratio (g/g) of 1:1, 1:3 and 3:1 respectively

Electron microscopy

TEM and SEM images of the synthesized magnetite (Fig. 1c and d) showed that magnetite NPs are spherical in shape with size ranging from 15 to 20 nm and are partially aggregated.

Immobilization of bacterial cells using magnetite NPs

Selected bacterial consortium gained magnetic properties via coating with magnetite NPs for 1 h. A schematic representation of immobilization process and digital photos for the separation of magnetite-bacterial consortium assembly are represented in Fig. 1D. Results revealed a proportional relation between coating efficiency and magnetite concentration reaching the highest efficiency (92%) at the highest magnetite ratio C (3:1 magnetite/bacterial cells) while the lowest coating efficiency of 46% was recorded at ratio B (1:3 magnetite/bacterial cells) after 1 h. After 15 h, coating efficiency of magnetite was slightly or not affected while coated bacteria were still having magnetic properties (Fig. 2).

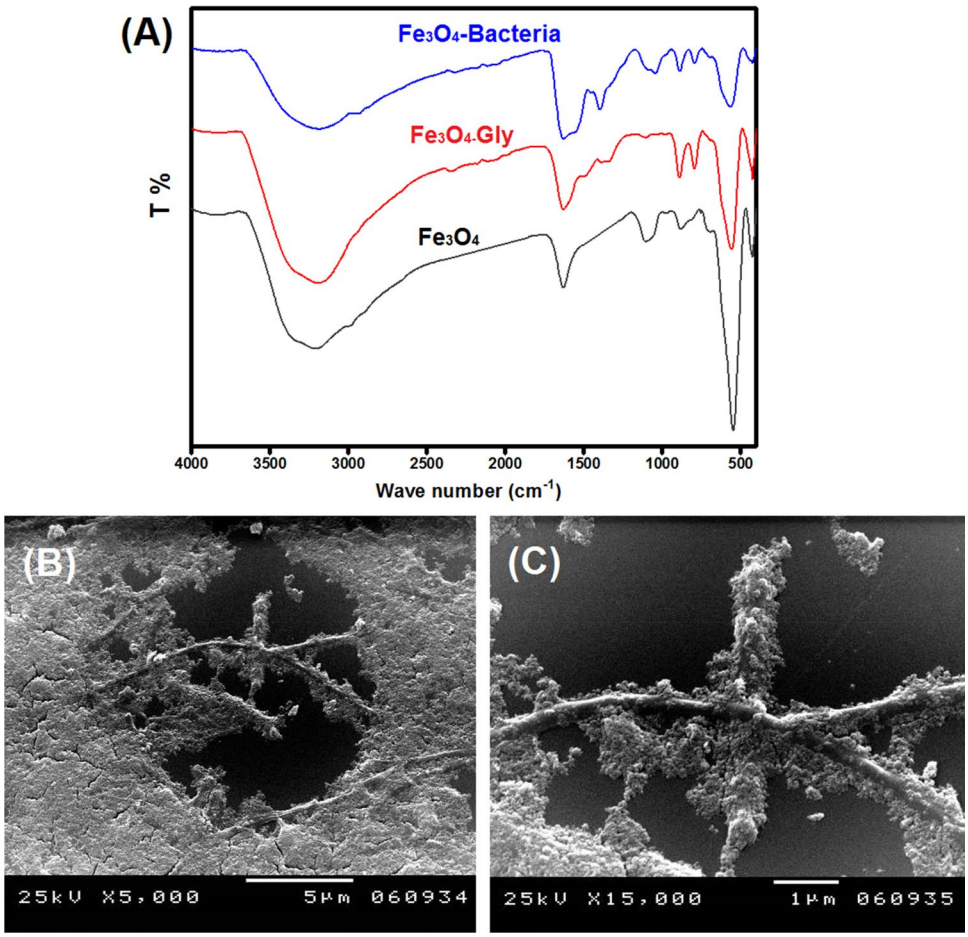

Fig. 3 FTIR spectra of Fe_3O_4, glycine coated Fe_3O_4 and glycine-Fe_3O_4-bacteria assembly (**a**) and SEM images of bacterial surface coated with magnetite (**b**, **c**)

Fourier transform infrared (FTIR)

Comparison between FTIR spectrum of magnetite modified with glycine before and after immobilization with bacteria is shown in Fig. 3A. The vibration at 547 cm^{-1} is corresponding to octahedral Fe–O stretching of the spinal Fe_3O_4 and absorption band around 3300 cm^{-1} is characteristic stretching vibration of hydroxyl group (H–O–H) on the surface of NPs or adsorbed water in the sample. The bending vibration of H–O–H group also localized at 1629 cm^{-1} indicated that glycine was successfully conjugated on the NPs. Coating of magnetite with glycine resulted in a broad absorption between 3000 and 3700 cm^{-1} which may be due the overlapping of O–H and N–H of the glycine. Moreover, new adsorption bands were observed at 2112 and 1385 cm^{-1} and the intensity of the band at 1629 cm^{-1} was significantly increased due to the presence of asymmetric stretching of carbonyl group C=O. Additional bands appeared at 1043, 1396, and 2927 cm^{-1} may indicate new functional groups from the immobilized bacteria.

Morphological characteristics of Fe_3O_4 NPs-immobilized bacterial cells

Selected bacterial consortium {*E. cloacae* NCDC279-56 (ATCC 13047) and *P. otitidis* MCC10330 (ATCC BAA-1130)} are rod-shaped cells that were immobilized by several layers of Fe_3O_4 NPs (Fig. 3b and c). The strong coverage is attributed to the size of the NPs (typically about 2 orders of magnitude smaller than the bacterial cell), which allows the attachment of multiple NPs onto a bacterial cell.

Bioremediation of oil hydrocarbons-contaminated effluent using Fe_3O_4

Bacteria assemblage

Fe_3O_4-bacteria assembly (3:1 w/w), a control culture (unseeded wastewater) and NPs free-mixed culture were investigated to decontaminate oily wastewater. Raw industrial wastewater recorded 616, 400.5, 1030, 247.6 and 1730 mg/l for O&G, TPH, TDS, TSS and COD respectively at the starting point. Results indicated significant differences ($P < 0.05$) among Fe_3O_4-immobilized bacteria, control and the Fe_3O_4-free mixed bacterial culture in the removal efficiency (RE %) and residual concentration (RC) of the tested parameters (Figs. 4 and 5 and supplementary data S2 A). Results revealed the following conclusions:

1. Fe_3O_4-coated bacteria achieved the highest TDS increases up to the first 4 h (84%, RC: 1895 mg/l) compared to the Fe_3O_4-free bacteria and the control which were still lower than its maximum permissible limit (MPL: 2000 mg/l) of the Egyptian Environmental Regulation Laws (No. 48/1982 and 4/1994) for safe discharge.
2. The highest RE(s) % of the TSS, COD, O&G and TPH were achieved by Fe_3O_4-coated bacteria (96, 65.4, 83.9 and 85%) after 4–24 h reaching RC(s) of 9.5, 598, 99 and 60 mg/l respectively. Compared with the MPLs of the tested parameters, TSS residue was much lower than its MPL (50 mg/l), highly compiled with environmental laws and therefore very safe for discharge into open environments. While COD, O&G and TPH were 5.98, 6.6, and 120 fold higher than their MPL(s) (100, 15 and 0.5 mg/l respectively).
3. Fe_3O_4-immobilized bacteria recorded significant differences ($P < 0.05$) in DO consumption compared to the Fe_3O_4-free bacteria and control.
4. Within the exposure duration (168 h), Fe_3O_4–immobilized bacteria exhibited significant relations between RE of the tested parameters and exposure time (S2 B). Significant ($P < 0.05$) relations between the removal of both O&G and TPH with time were recorded reaching the lowest RCs (99 and 60 mg/l) of the two parameters respectively after 24 h. Similarly significant ($P < 0.05$) DO consumption, COD removal and TDS increase were recorded with time reaching the highest after 24 h while lowest RC of TSS was observed until the 4th h. The Fe_3O_4-immobilized assemblage exhibited exothermic activity and recording significant temperature differences after the 4th h ($a = 24$ C°).
5. Although the highest removals of the tested parameters were recorded after 24 h, it is preferred to stop the experiment at 4 h (S2 B).

Multifactorial analysis (Pearson Correlations) revealed several correlations among the different tested contaminants presented in the petroleum hydrocarbon contaminated effluents during Fe_3O_4 -immobilized bacteria treatment (S2 C). Highly significant positive correlations (at $P < 0.01$) were detected among O&G TPH, TSS and COD, all of which had highly significant negative correlations with temperature and TDS. DO showed highly significant negative correlations (at $P < 0.01$) with TDS and COD, while showed no correlations with other parameters.

Effect of Fe_3O_4 NPs on the bacterial growth after immobilization and during the bioremediation process

After immobilization, magnetite NPs enhanced bacterial growth rate (measured as optical density, OD) in the growth medium with increasing magnetite concentration reaching the highest growth rate at magnetite to bacterial cells ratio C of 3:1 (w/w) during the first 4 h recording 5.07 fold higher

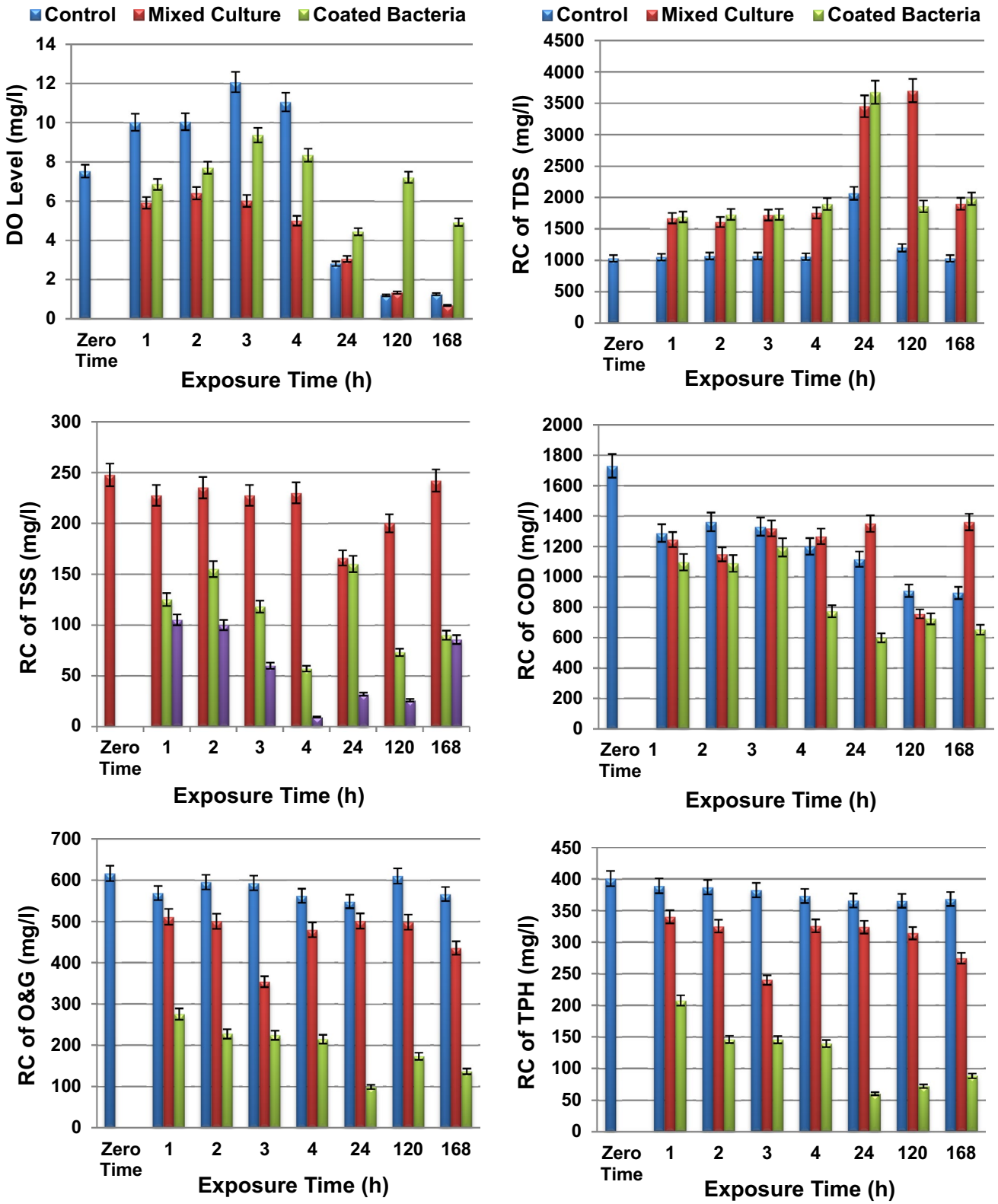

Fig. 4 Residual concentrations of different parameters before and after treatment using free living- mixed culture and Fe_3O_4-coated bacteria

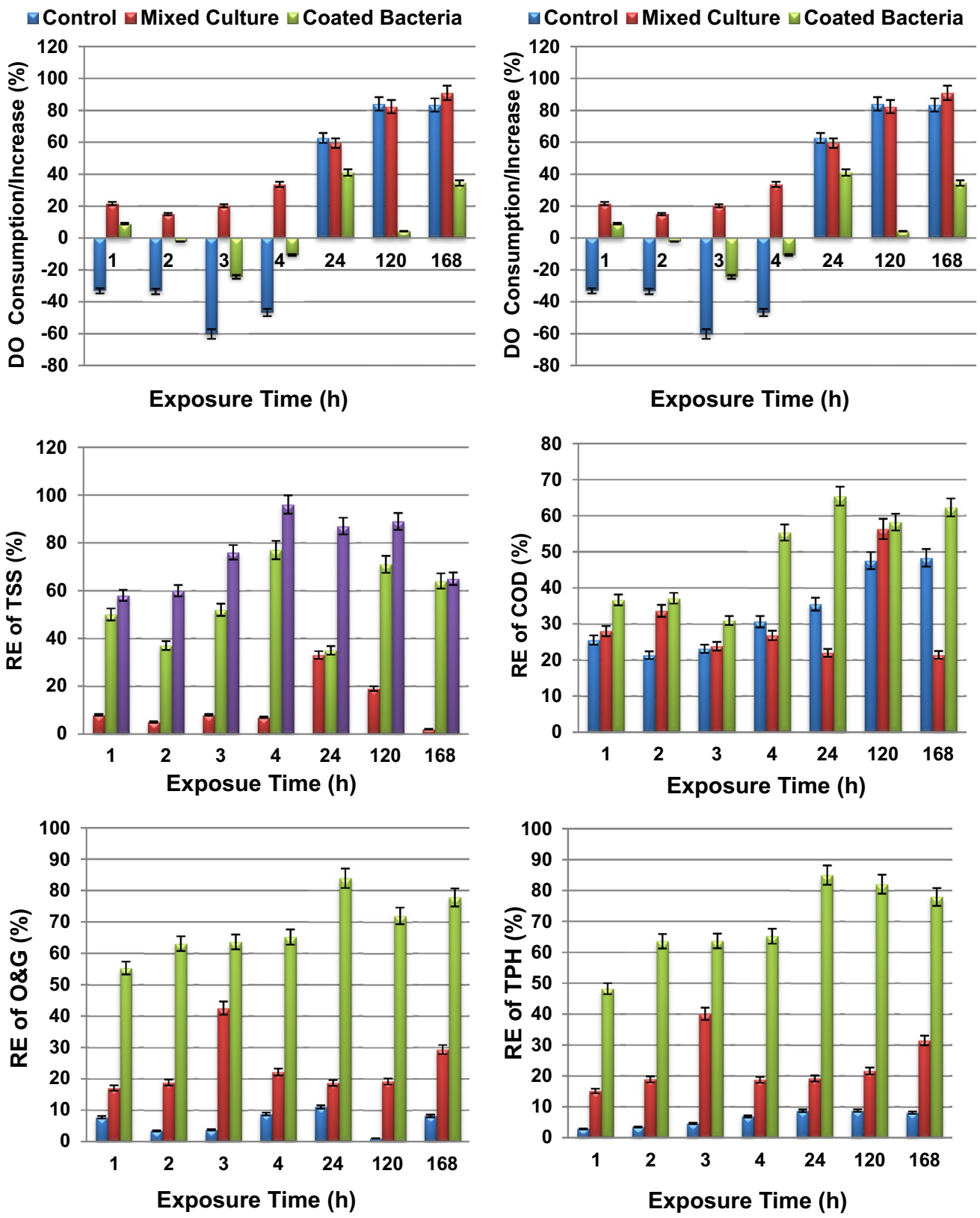

Fig. 5 Removal efficiencies of different parameters before and after treatment using free living-mixed culture and Fe_3O_4-coated bacteria

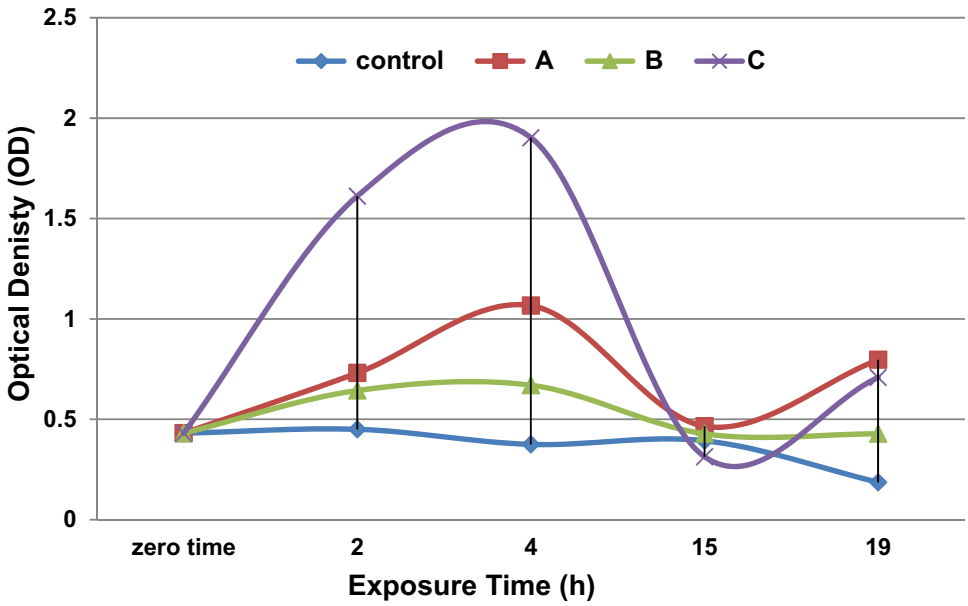

Fig. 6 Effect of magnetite NPs on the growth rate of the mixed culture with and without magnetite NPs

than the control (free cells) followed by ratios A and then B (Fig. 6).

During the treatment process, the highest growth rate was achieved by the control culture (0.2802 OD) after 1 h that is equivalent to 2.3 folds higher biomass density compared to the initial biomass which is followed by regular growth decline indicating high toxicity of wastewater against the indigenous bacteria. Upon incubation of Fe_3O_4-bacterial culture with the raw wastewater, the highest growth was recorded after 168 h (0.4191 OD), equivalent to 1.9 fold higher biomass density compared to the initial density at the starting point (Fig. 7). The mixed culture recorded its highest growth (0.3599 OD) after 24 h, equivalent to 1.5 fold higher than the initial biomass. Such results confirmed the regular ascending stimulation effects of the nanoparticles on the growth and multiplication of the tested bacteria till the end of the experiment.

Treatment using magnetite NPs

Role of magnetite nanoparticles only in the treatment of oily wastewater was compared with the role magnetite NPs-microbial cells assembly (Fig. 8). Fe_3O_4-immobilized

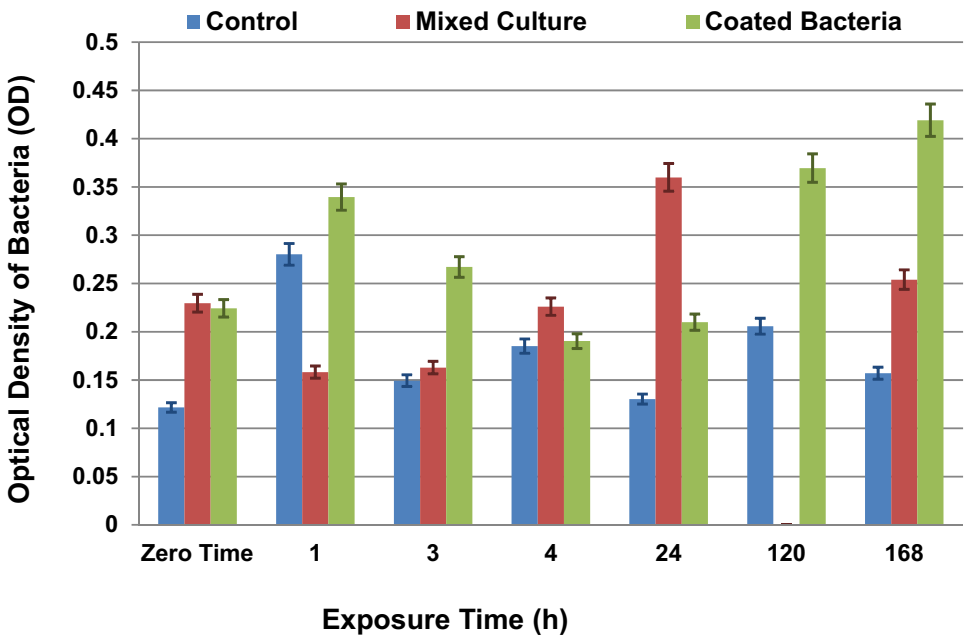

Fig. 7 Stimulatory and/or inhibitory effects of tested wastewater on the growth of the selected bacteria during the Fe_3O_4-bacteria bioassay

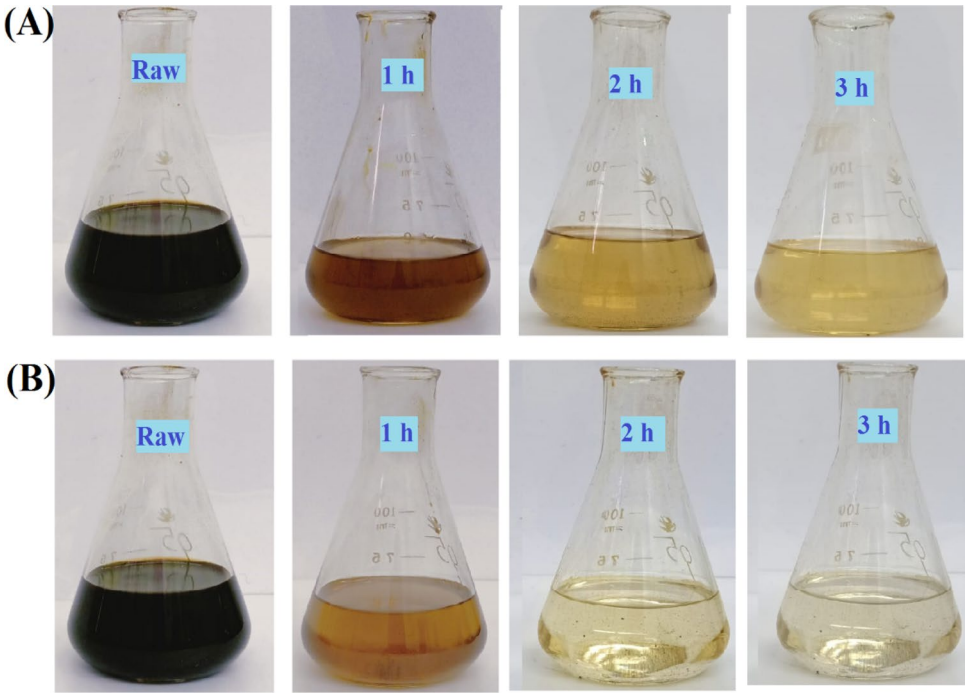

Fig. 8 Digital photos for the residual concentration of O&G before and after the treatment using magnetite NPs (**a**) and Fe_3O_4-immobilized bacteria (**b**)

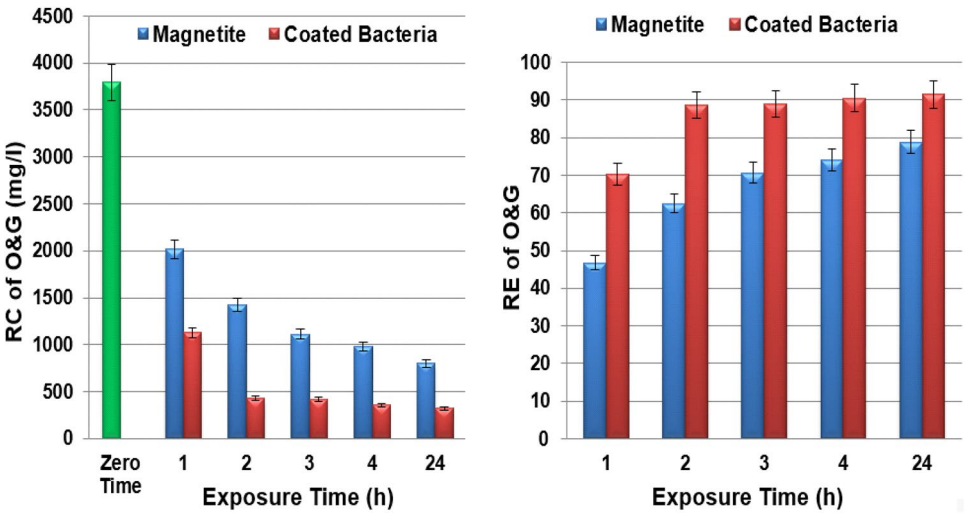

Fig. 9 Residual concentration and removal efficiency of O&G from wastewater treated by Fe_3O_4 NPs and Fe_3O_4-coated bacteria

bacteria recorded the highest removal efficiency for both TPH and O&G after 24 h compared to treatment using the magnetite only during all the experimental exposure times (Figs. 9 and 10). These results confirmed the critical role played by Fe_3O_4-immobilized bacteria assembly in the treatment of hydrocarbons-contaminated wastewater.

These results clearly indicated that bacteria free-nanoparticles (chemical removal) could efficiently remove organic contaminants by adsorption process. However, a significant improvement of oily wastewater bioremediation was obtained by combining magnetite and bacterial cells. These results are in agreement with those recorded previously for biodesulfurization using bacterial cells immobilized with γ-Al_2O_3 Nano sorbents. γ-Al_2O_3 Nano sorbents only adsorbed DBT on its surface till all the pores were saturated. While with bacterial assembly, γ-Al_2O_3 Nano sorbents could accelerate the DBT transfer from the aqueous phase to the microbial cell surfaces which increased the desulfurization. As mentioned before, very small size nanoparticles (10 nm or less in diameter) or 20 nm are not only adsorbed on the surface of cells, but also entered into the interior of cells when the magnetic cells left in the suspension for 3 h. After 6 h, cells are destroyed and deformed by the concentrated nanoparticles in the suspension. So, the present results recommend running the experiment for 4 h with multiple Fe_3O_4-immobilized bacterial cultures in

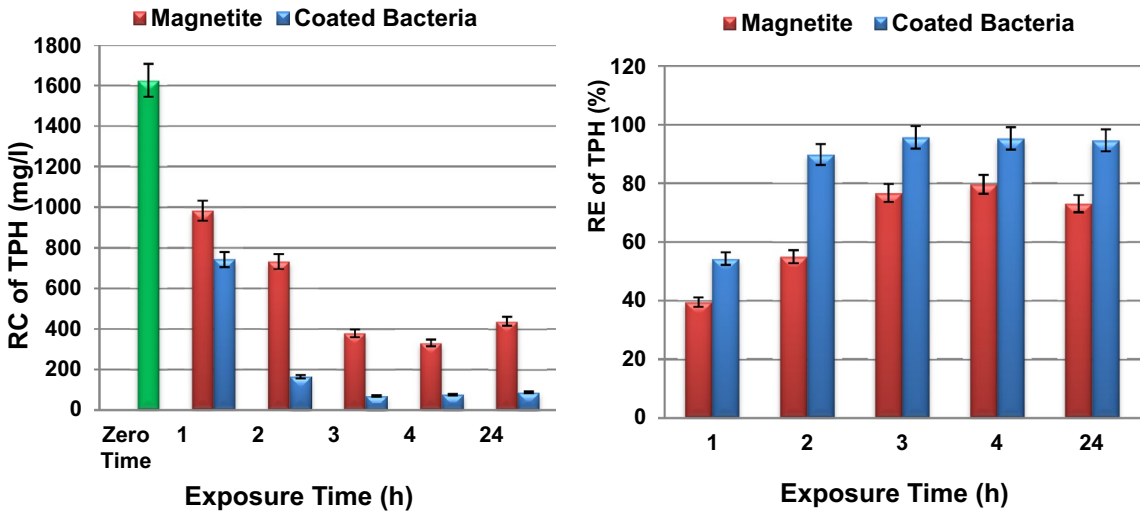

Fig. 10 Residual concentration and removal efficiency of TPH from wastewater treated by Fe_3O_4 NPs and Fe_3O_4-coated bacteria

sequence. Although the highest removal efficiency of the main parameters (O&G, TPH and COD) were achieved after only 24 h, they still higher than their MPLs. Using multiple Fe_3O_4-immobilized bacterial cultures in sequence will help reaching the required MPLs, saving time, energy and preventing the probability of abnormal cell function or death due to the presence of magnetite for a long time. It is also recommended to carry physical pre-treatment step prior to the treatment with Fe_3O_4-bacteria assembly.

Discussion

The marvellous biodegradation activity possessed by the selected microbial cells (*Enterobacter cloacae* NCDC279-56 and *Pseudomonas otitidis* MCC10330) especially as a consortium was reported in a previous study by the authors and by other workers (Das and Chandran 2011; Sarafzadeh et al. 2013). This activity is attributed mainly to their enzymatic capacities coupled with their ability to produce bioactive compounds such as biosurfactants and bioflocculants that greatly aid in the degradation and removal of oil hydrocarbons among other contaminants in the wastewater (Sathishkumar et al. 2008; Meng et al. 2018; Xia et al. 2019).

Characterization of magnetic NPs

Magnetite was selected due to its compatibility (nontoxic) to the tested bacteria and wide applications in biomedical field. Besides, glycine was used as a surfactant where its carboxylic groups (COOH) react with the positively charged magnetite as well as with a large number of hydroxyl groups on its surface (Bruno et al. 2018). H–O–H group localized at 1629 cm^{-1} of the FTIR spectrum of magnetite confirmed that glycine was successfully conjugated on the NPs (El-Subruiti et al. 2019). Glycine produces an amine layer on the surface of magnetite NPs, which leads to stabilization in the dispersion of magnetite NPs in water phase with hydrophilic characteristics, preventing their aggregation and help formation of Fe_3O_4 NPs with smaller sizes (Viota et al. 2010; Bardania et al. 2013). The new adsorption bands at 2112 and 1385 cm^{-1} are related to N–H stretching and symmetric stretching of C=O (Mailoud et al. 2018; Schwaminger et al. 2015) while bands appeared at 1043, 1396, and 2927 cm^{-1} could be attributed to the presence of new functional groups from the immobilized bacteria (Wang et al. 2017). TEM image showed that particles are partially aggregated, which is attributed to the superparamagnetic behaviour of the synthesized nanoparticles (Wu et al. 2010; Sallam et al. 2018). According to the coercivity (Hc, 0.30 emu/g), the prepared magnetite NPs were found to have superparamagnetic behaviour. It has been reported that iron oxides NPs with a high value of Hc are called ferromagnetic or ferrimagnetic at room temperature, whereas those with a low value (lower than 20 Oe) are called superparamagnetic (Alizadeh et al. 2012; El-Subruiti et al. 2019).

Immobilization of bacterial cells using magnetite NPs

NP association with biomass is likely takes place on one or two general steps. The first step is adsorption of NPs to extracellular polymeric substances (EPS) or the cell surface.

The adsorption mechanism (decoration) was considered to be mainly by electrostatic attraction between the negative charges on the surface of bacterial cells, and the positive charges of glycine coated magnetite NPs. In addition, the presences of a variety of functional groups on microbial cell surface interact with the modified Fe_3O_4 NPs where the large specific surface area and high surface energy of the NPs make the adsorption even stronger (Li et al. 2009; Boniek et al. 2015). After adsorption to the cell surface, the second step is the uptake or penetration into the cell depends on the size of NPs. It was reported that NPs of 10 nm or less in diameter could penetrate bacterial cell membrane and damage the cells or lead to abnormal cell functions, whereas larger NPs such as those in the present study do not (Choi and Hu 2008; Kiser et al. 2010). However, NPs found suitable with diameter up to 50 nm but in case particles larger than 50 nm, their Brownian energy overwhelms the relatively weak attachment forces as shown with other workers (Ansari et al. 2009).

Effect of Fe_3O_4 NPs on the bacterial growth before and during treatment process

Enhancement of bacterial growth rate with increasing magnetite concentration especially at magnetite to bacterial cells ratio C (3:1 w/w) reaching 5.07 fold higher than the control was supported by other workers who reported growth enhancement up to 500 ppm magnetite NPs (Kafayati et al. 2013; Konate et al. 2018). It was also proved that the 3:1 ratio (magnetite NPs: bacteria) resulted in the highest values of biomass recovery for the *R. erythropolis* FMF cells (Bardania et al. 2013).

During the treatment process, raw wastewater exhibited high toxicity to the indigenous bacteria of the control after the first treatment hour with regular growth decline till the end of the experiment duration. However, Fe_3O_4-bacterial culture biomass showed continuous increase till the last exposure reaching the highest growth (1.9 fold higher biomass density than the initial) after 168 h while the Fe_3O_4-free bacterial culture showed lower (1.5 fold) growth biomass compared to the start up density. Such results confirmed the regular ascending stimulation effects of the nanoparticles on the growth and multiplication of the tested bacteria till the end of the experiment. This is attributed to the fact magnetic NPs with a super paramagnetic behaviour such as Fe_3O_4 used in the present study have very low toxicity on the living cells (Samanta et al. 2008). Moreover, glycine modified magnetite NPs with different surfactants also showed negligible toxicity on eukaryote cells compared to free NPs (Kafayati et al. 2013; Mahmoudi et al. 2009 and 2011). Besides, ease of separation and microbial longevity are advantages of bacterial immobilization (Ansari et al. 2009; Shan et al. 2005).

Bioremediation of oil hydrocarbons—contaminated effluent using Fe_3O_4-bacteria Assemblage

Although using free dispersed bacteria optimizes their mass transport, it is difficult to be separated from the reaction medium after treatment or may lead to their death, thus, bacterial immobilization as biofilms is a good solution (Khan et al. 2019; Liu et al. 2019a). Immobilization of bacteria offers treatment system with high activity, high tolerance against toxic chemicals and high resistance to pH and temperature changes as well as other environmental stresses (Shin et al. 2002). Also, immobilized bacterial assemblage systems facilitate utilization of biomass, liquid/solid separation and minimize blocking of continuous-flow systems (Xu et al. 2012). Entrapment (immobilization) technique of bacteria suffers many limitations such as mass transfer problems that limit the access to the substrate (Xu et al. 2006; Jia et al. 2019) which can be eliminated by bacterial immobilization through adsorption technique which is much simpler but is limited by biomass loading, stability during operation, and the adhesion strength between bacteria and nanoparticles (Yu et al. 2017). In order to combine the advantages of immobilization (ease of separation and microbial longevity) with those of free dispersal (good mass transport) another approach was adopted where selected bacterial cells were immobilized (coated) with magnetic NPs (Ansari et al. 2009). Immobilization using magnetic NPs has the advantage of experiencing minimal mass transfer problems as well as possibility to concentrate the dispersed coated cells by application of an external magnetic field to reuse them without centrifugation or microbial death (Shan et al. 2005).

Iron oxide NPs with its chemical inertness and biocompatibility have high potential for biomass immobilization where they stimulate microbial activity and reaction rates besides being simplest method for oil removal by physical adsorption. In the present study, magnetite NPs-immobilized bacterial assemblage greatly enhanced bioremediation of hydrocarbons contaminated wastewater compared to NPs-free bacteria (He et al. 2017; Wu et al. 2018). These results are in agreement with those of Ansari et al. (2009) and Guobin et al. (2005) who used *Rhodococcus erythropolis* IGTS8 coated with glycine-modified Fe_3O_4 NPs and *Pseudomonas delafieldii* and *R. erythropolis* LSSE8-1 with ammonium oleate modified Fe_3O_4 NPs respectively.

Biological treatment associated with NPs positively enhanced the treatment efficiency compared to NPs-free biological systems, saved time and can reduce energy costs when apply at an industrial scale. In the present study, the highest O&G, TPH removals were achieved by Fe_3O_4-immobilized bacteria after 24 h only indicating that Fe_3O_4NPs could serve as a facilitator in microbial

remediation of contaminants by enhancing their growth, immobilizing the remediating agents, induction of remediating microbial enzymes or biosurfactants as well as solving problems associated with petroleum hydrocarbons' reduced solubility and bioavailability to microorganisms and hazardous effects on microbial viability. Moreover, nanotechnology can be considered as an effective tool to facilitate bioremediation of persistent hydrophobic toxicants and augment the process through adsorption of wastes on nanoparticles surfaces which also has a role in the treatment.

Conclusions

In conclusion, the proposed Fe_3O_4-bacterial assembly system proved to be a very efficient for the treatment of highly polluted petroleum hydrocarbons wastewater considering the very short running time. It is recommended using multiple Fe_3O_4-immobilized bacterial cultures in sequence (each for 4 h) although the highest removal efficiency of O&G, TPH and COD were achieved after 24 h. Using multiple Fe_3O_4-immobilized bacterial cultures in sequence will help reaching the required MPLs, saving time, energy and preventing the probability of abnormal cell functions or death due to the presence of magnetite for a long time. It is also recommended to carry physical pre-treatment step prior to the treatment with Fe_3O_4-bacteria assembly.

Compliance with ethical standards

Conflict of interest All authors declare that they have no conflict of interest. This article does not contain any studies with animals performed by any of the authors.

References

Abdelwahab O, Amin N, El-Ashtoukhy EZ (2009) Electrochemical removal of phenol from oil refinery wastewater. J Hazard Mater 163:711–716

Al Zarooni M, Elshorbagy W (2006) Characterization and assessment of Al Ruwais refinery wastewater. J Hazard Mater 136:398–405

Alizadeh A, Khodaei MM, Beygzadeh M, Kordestani D, Feyzi M (2012) Biguanide-functionalized Fe_3O_4/SiO_2 magnetic nanoparticles: an efficient heterogeneous organosuperbase catalyst for various organic transformations in aqueous media. Bull Korean Chem Soc 33:2546–2552

Altaş L, Büyükgüngör H (2008) Sulfide removal in petroleum refinery wastewater by chemical precipitation. J Hazard Mater 153:462–469

Ansari F, Grigoriev P, Libor S, Tothill IE, Ramsden JJ (2009) DBT degradation enhancement by decorating *Rhodococcus erythropolis* IGST8 with magnetic Fe_3O_4 nanoparticles. Biotechnol Bioeng 102(5):1505–1512

Baghaie AH, Jabari AG (2019) Effect of nano Fe-oxide and endophytic fungus (*P. indica*) on petroleum hydrocarbons degradation in an arsenic contaminated soil under barley cultivation. J Environ Health Sci Eng 1–9

Bardania H, Raheb J, Mohammad-Beigi H, Rasekh B, Arpanaei A (2013) Desulfurization activity and reusability of magnetite nanoparticle–coated *Rhodococcus erythropolis* FMF and *R. erythropolis* IGTS8 bacterial cells. Biotechnol Appl Biochem 60(3):323–329

Boniek D, Figueiredo D, dos Santos AFB, de Resende Stoianoff MA (2015) Biodesulfurization: a mini review about the immediate search for the future technology. Clean Technol Environ Policy 17:29–37

Bruno A, Correa J, Peláez-Abellán E, Urones-Garrote E (2018) A novel method for the functionalization of aminoacids L-glycine, L-glutamic acid and L-arginine on maghemite/magnetite nanoparticles. J Magn Magn Mater 456:87–91

Changmai M, Pasawan M, Purkait M (2019) Treatment of oily wastewater from drilling site using electrocoagulation followed by microfiltration. Sep Purif Technol 210:463–472

Chen J, Liu S, Qi X, Yan S, Guo Q (2018) Study and design on chemical oxygen demand measurement based on ultraviolet absorption. Sens Actuat B Chem 254:778–784

Chen M, Zhu L, Chen J, Yang F, Tang CY, Guiver MD, Dong Y (2020) Spinel-based ceramic membranes coupling solid sludge recycling with oily wastewater treatment. Water Res 169:115180

Choi O, Hu Z (2008) Size dependent and reactive oxygen species related nanosilver toxicity to nitrifying bacteria. Environ Sci Technol 42:4583–4588

Clesceri L, Greenberg A, Eaton A (1999) Standard methods for the examination of water and wastewater, 20th edn. American Public Health Association, American Water Work Association, Water Environment Federation, Washington, DC, APHA-AWWA-WEF

Crini G, Lichtfouse E (2019) Advantages and disadvantages of techniques used for wastewater treatment. Environ Chem Lett 17:145–155

Darabdhara G, Boruah PK, Hussain N, Borthakur P, Sharma B, Sengupta P, Das MR (2017) Magnetic nanoparticles towards efficient adsorption of gram positive and gram negative bacteria: an investigation of adsorption parameters and interaction mechanism. Colloids Surf Physicochem Eng Aspects 516:161–170

Das N, Chandran P (2011) Microbial degradation of petroleum hydrocarbon contaminants: an overview. Biotechnol Res Int. https://doi.org/10.4061/2011/941810

Diya'uddeen BH, Daud WMAW, Aziz AA (2011) Treatment technologies for petroleum refinery effluents: a review. Process Saf Environ Prot 89:95–105

El Bestawy E, Ahmed A-H, Amer R, Kashmeri RA (2014) Decontamination of domestic wastewater using suspended individual and mixed bacteria in batch system. J Bioremed Biodegred 5:1

El-Bestawy E, El-KHeir EA, El-Fatah HA, Hassouna S (1998) Enhancement of bacterial efficiency for metal removal using mutation techniques. World J Microbiol Biotechnol 14:853–856

El-Boubbou K, Gruden C, Huang X (2007) Magnetic glyco-nanoparticles: a unique tool for rapid pathogen detection, decontamination, and strain differentiation. J Am Chem Soc 129(44):13392–13393

El-Subruiti G, Eltaweil A, Sallam S (2019) Synthesis of active MFe_2O_4/γ-Fe_2O_3 nanocomposites (metal = Ni or Co) for reduction of nitro-containing pollutants and methyl orange degradation. NANO 14:1950125

Escobar AM, Blanco MN, Martínez JJ, Cubillos JA, Romanelli GP, Pizzio LR (2019) Biomass derivative valorization using nano core-shell magnetic materials based on keggin-heteropolyacids: levulinic acid esterification kinetic study with n-butanol. J Nanomater 2019

Gubin SP, Koksharov YA, Khomutov G, Yurkov GY (2005) Magnetic nanoparticles: preparation, structure and properties. Russ Chem Rev 74:489

Guobin S, Huaiying Z, Weiquan C, Jianmin X, Huizhou L (2005) Improvement of biodesulfurization rate by assembling nanosorbents on the surfaces of microbial cells. Biophys J 89(6):L58–L60

He K, Chen G, Zeng G, Huang Z, Guo Z, Huang T, Peng M, Shi J, Hu L (2017) Applications of white rot fungi in bioremediation with nanoparticles and biosynthesis of metallic nanoparticles. Appl Microbiol Biotechnol 101:4853–4862

Henshaw PF, Zhu W (2001) Biological conversion of hydrogen sulphide to elemental sulphur in a fixed-film continuous flow photoreactor. Water Res 35:3605–3610

Hou J, Liu F, Wu N, Ju J, Yu B (2016) Efficient biodegradation of chlorophenols in aqueous phase by magnetically immobilized aniline-degrading *Rhodococcus rhodochrous* strain. J Nanobiotechnol 14:5

Jia X, Zhang S, Li J, Xia J, Yao R, Zhao X, Wu B, Bai F, Xiao Y (2019) Engineered bacterial biofloc formation enhancing phenol removal and cell tolerance. Appl Microbiol Biotechnol 1–13

Kafayati ME, Raheb J, Torabi Angazi M, Alizadeh S, Bardania H (2013) The effect of magnetic Fe_3O_4 nanoparticles on the growth of genetically manipulated bacterium, *Pseudomonas aeruginosa* (PTSOX4). Iran J Biotechnol 11(1):41–46

Kalfa OM, Yalçınkaya Ö, Türker AR (2009) Synthesis of nano B_2O_3/TiO_2 composite material as a new solid phase extractor and its application to preconcentration and separation of cadmium. J Hazard Mater 166:455–461

Katam K, Bhattacharyya D (2019) Simultaneous treatment of domestic wastewater and bio-lipid synthesis using immobilized and suspended cultures of microalgae and activated sludge. J Ind Eng Chem 69:295–303

Khan F, Lee J-W, Pham DTN, Lee J-H, Kim H-W, Kim Y-K, Kim Y-M (2019) Streptomycin mediated biofilm inhibition and suppression of virulence properties in *Pseudomonas aeruginosa* PAO1. Appl Microbiol Biotechnol 1–18

Kiser MA, Ryu H, Jang H, Hristovski K, Westerhoff P (2010) Biosorption of nanoparticles to heterotrophic wastewater biomass. Water Res 44:4105–4114

Konate A, Wang Y, He X, Adeel M, Zhang P, Ma Y, Ding Y, Zhang J, Yang J, Kizito S (2018) Comparative effects of nano and bulk-Fe_3O_4 on the growth of cucumber (*Cucumis sativus*). Ecotoxicol Environ Saf 165:547–554

Kumari B, Singh D (2016) A review on multifaceted application of nanoparticles in the field of bioremediation of petroleum hydrocarbons. Ecol Eng 97:98–105

Li Y-G, Gao H-S, Li W-L, Xing J-M, Liu H-Z (2009) In situ magnetic separation and immobilization of dibenzothiophene-desulfurizing bacteria. Bioresour Technol 100(21):5092–5096

Liu Y, Feng H, Fu R, Zhang N, Du W, Shen Q, Zhang R (2019a) Induced root-secreted d-galactose functions as a chemoattractant and enhances the biofilm formation of *Bacillus velezensis* SQR9 in an McpA-dependent manner. Appl Microbiol Biotechnol 1–13

Liu Y, Wang W, Shah SB, Zanaroli G, Xu P, Tang H (2019b) Phenol biodegradation by *Acinetobacter radioresistens* APH1 and its application in soil bioremediation. Appl Microbiol Biotechnol 1–11

Mahmoudi M, Simchi A, Milani A, Stroeve P (2009) Cell toxicity of superparamagnetic iron oxide nanoparticles. J colloid Interface Sci 336(2):510–518

Mahmoudi M, Shokrgozar MA, Sardari S, Moghadam MK, Vali H, Laurent S, Stroeve P (2011) Irreversible changes in protein conformation due to interaction with superparamagnetic iron oxide nanoparticles. Nanoscale 3(3):1127–1138

Mailoud OM, Elsayed AH, Abo-Elazm A, Fetouh H (2018) Synthesis and study the structure, optical, thermal and dielectric properties of promising glycine copper nitrate (GCN) single crystals. Results Phys 10:512–520

Meng L, Bao M, Sun P (2018) Construction of long-chain alkane degrading bacteria and its application in bioremediation of crude oil pollution. Int J Biol Macromol 119:524–532

Pardeshi S, Patil A (2008) A simple route for photocatalytic degradation of phenol in aqueous zinc oxide suspension using solar energy. Sol Energy 82:700–705

Polak J, Lu BC-Y (1973) Mutual solubilities of hydrocarbons and water at 0 and 25 °C. Can J Chem 51:4018–4023

Poulopoulos S, Voutsas E, Grigoropoulou H, Philippopoulos C (2005) Stripping as a pretreatment process of industrial oily wastewater. J Hazard Mater 117:135–139

Qiao N, Gao M, Zhang X, Du Y, Fan X, Wang L, Liu N, Yu D (2019) Trichosporon fermentans biomass flocculation from soybean oil refinery wastewater using bioflocculant produced from *Paecilomyces* sp. M2-1. Appl Microbiol Biotechnol 103:2821–2831

Raee MJ, Ebrahiminezhad A, Ghoshoon MB, Gholami A, Ghasemi Y (2019) Synthesis and characterization of L-lysin coated iron oxide nanoparticles as appropriate choices for cell immobilization and magnetic separation. Nanosci Nanotechnol-Asia 9:462–466

Ranmadugala D, Ebrahiminezhad A, Manley-Harris M, Ghasemi Y, Berenjian A (2018) Magnetic immobilization of bacteria using iron oxide nanoparticles. Biotechnol Lett 40:237–248

Rathnayake D, Sathasivan A, Kastl G, Krishna KB (2019) Hydrogen sulphide control in sewers by catalysing the reaction with oxygen. Sci Total Environ 689:1192–1200

Reddy LH, Arias JL, Nicolas J, Couvreur P (2012) Magnetic nanoparticles: design and characterization, toxicity and biocompatibility, pharmaceutical and biomedical applications. Chem Rev 112:5818–5878

Sallam S, El-Subruiti G, Eltaweil A (2018) Facile synthesis of Ag-γ-Fe_2O_3 superior nanocomposite for catalytic reduction of nitroaromatic compounds and catalytic degradation of methyl orange. Catal Lett 148:3701–3714

Samanta B, Yan H, Fischer NO, Shi J, Jerry DJ, Rotello VM (2008) Protein-passivated Fe_3O_4 nanoparticles: low toxicity and rapid heating for thermal therapy. J Mater Chem 18(11):1204–1208

Sarafzadeh P, Hezave AZ, Ravanbakhsh M, Niazi A, Ayatollahi S (2013) *Enterobacter cloacae* as biosurfactant producing bacterium: differentiating its effects on interfacial tension and wettability alteration mechanisms for oil recovery during MEOR process. Colloids Surf B Biointerfaces 105:223–229

Sathishkumar M, Binupriya AR, Baik SH, Yun SE (2008) Biodegradation of crude oil by individual bacterial strains and a mixed bacterial consortium isolated from hydrocarbon contaminated areas. Clean-Soil Air Water 36:92–96

Schwaminger SP, García PF, Merck GK, Bodensteiner FA, Heissler S, Günther S, Berensmeier S (2015) Nature of interactions of amino acids with bare magnetite nanoparticles. J Phys Chem C 119:23032–23041

Shan G, Xing J, Zhang H, Liu H (2005) Biodesulfurization of dibenzothiophene by microbial cells coated with magnetite nanoparticles. Appl Environ Microbiol 71(8):4497–4502

Shin M, Nguyen T, Ramsay J (2002) Evaluation of support materials for the surface immobilization and decoloration of amaranth by *Trametes versicolor*. Appl Microbiol Biotechnol 60:218–223

Soares-Castro P, Yadav TC, Viggor S, Kivisaar M, Kapley A, Santos PM (2019) Seasonal bacterial community dynamics in a crude oil refinery wastewater treatment plant. Appl Microbiol Biotechnol 103:9131–9141

Stoll U, Gupta H (1997) Management strategies for oil and grease residues. Waste Manage Res 15:23–32

Sulistyaningsih T, Santosa SJ, Siswanta D, Rusdiarso B (2017) Synthesis and characterization of magnetites obtained from mechanically

and sonochemically assissted co-precipitation and reverse co-precipitation methods. Int J Mater Mech Manuf 5:16–19

Sze K, Lu Y, Wong P (1997) Removal and recovery of copper ion (Cu^{2+}) from electroplating effluent by a bioreactor containing magnetite-immobilized cells of *Pseudomonas putida* 5X. Stud Environ Sci 66:131–149

Tanudjaja HJ, Hejase CA, Tarabara VV, Fane AG, Chew JW (2019) Membrane-based separation for oily wastewater: a practical perspective. Water Res 156:347–365

Viota J, Arroyo F, Delgado A, Horno J (2010) Electrokinetic characterization of magnetite nanoparticles functionalized with amino acids. J Colloid Interface Sci 344:144–149

Wang Z, Fingas M (1995) Differentiation of the source of spilled oil and monitoring of the oil weathering process using gas chromatography-mass spectrometry. J Chromatogr 712:321–343

Wang Y-D, Li X-L, Liu Z-X, Zhang X-X, Hu J, Lü J-H (2017) Discrimination of foodborne pathogenic bacteria using synchrotron FTIR microspectroscopy. Nucl Sci Technol 28:49

Wu C, He H, Gao H, Liu G, Ma R, An Y, Shi L (2010) Synthesis of Fe_3O_4@ SiO_2@ polymer nanoparticles for controlled drug release. Sci China Chem 53:514–518

Wu X, He H, Yang WL, Yu J, Yang C (2018) Efficient removal of atrazine from aqueous solutions using magnetic *Saccharomyces cerevisiae* bionanomaterial. Appl Microbiol Biotechnol 102:7597–7610

Xia M, Fu D, Chakraborty R, Singh RP, Terry N (2019) Enhanced crude oil depletion by constructed bacterial consortium comprising bioemulsifier producer and petroleum hydrocarbon degraders. Bioresour Technol 282:456–463

Xu X, Zhu X (2004) Treatment of refectory oily wastewater by electrocoagulation process. Chemosphere 56:889–894

Xu P, Yu B, Li FL, Cai XF, Ma CQ (2006) Microbial degradation of sulfur, nitrogen and oxygen heterocycles. Trends Microbiol 14:398–405

Xu P, Zeng GM, Huang DL, Feng CL, Hu S, Zhao MH, Lai C, Wei Z, Huang C, Xie GX (2012) Use of iron oxide nanomaterials in wastewater treatment: a review. Sci Total Environ 424:1–10

Yu L, Han M, He F (2017) A review of treating oily wastewater. Arabian J Chem 10:S1913–S1922

Yu L, Yang Y, Yang B, Li Z, Zhang X, Hou Y, Lei L, Zhang D (2018) Effects of solids retention time on the performance and microbial community structures in membrane bioreactors treating synthetic oil refinery wastewater. Chem Eng J 344:462–468